APPLICATION OF H-BRIDGE VOLTAGE SOURCE INVERTER TOPOLOGY WITH PROPORTIONAL INTEGRAL CONTROLLER IN A PHOTOVOLTAIC POWER CONDITIONING SYSTEM

DIYOKE G. C.[1*], OBI P. I.[1] AND ONWUKA I. K.[1]
[1] Michael Okpara University of Agriculture, Umudike, P.M.B 7267 Umuahia, Abia State, Nigeria.
*Corresponding Author: geraldiyoke@mouau.edu.ng

ABSTRACT: *- This paper proposes an application of H-bridge voltage source inverter topology with proportional integral controller in a photovoltaic power conditioning system. A very crucial part of power conditioning system (PCS) for energy sustainability is photovoltaic (PV) dc/ac converter. The H-bridge dc/ac converter is provided to regulate the constant output voltage under various operating conditions of photovoltaic cell. The power rating of power switch (MOSFET) for dc/ac converter is selected on the basis of photovoltaic cell's maximum output power. PV power conditioning system should have high efficiency under different irradiance values to satisfy the system operating conditions. An H-bridge converter topology is proposed to satisfy PV PCS conditions with inclusion of feedback system. The performance of the system was studied through simulation in MATLAB/SIMULINK/simpowersystems. As a result of the feedback system, a constant output power of 780 Watts, constant load voltage of 280 V, high efficiency value of 99.49 % were achieved with low total harmonic distortion (THD) value of 0.97 % obtained.*

Keywords: H-bridge inverter, photovoltaic cell, proportional integral (PI) controller, power conditioning, unipolar pulse width modulation.

1. INTRODUCTION

The renewable energy application for sustainability of energy demand has increased due to continuous growth in energy consumption and the continuously decaying fossil fuels (NingYi, et al., 2014, Ansari, et al., 2010, Nagaiah, et al., 2017, Sujatha, et al., 2019 and Brunton, et al., 2010). Due to its zero pollution (both air and noise), photovoltaic (PV) power has been a promising and reliable form renewable energy source in the world today. The ability to operate with much less restriction on location, and ease of maintenance has made it more popular (Chen, et al., 2010, Adelakun, et al., 2019, Gul et al., 2016 and Juraz, et al., 2020). Due to inherent merits (Abolhosseini, et al., 2020, Emeghara, et al., 2022 and Kumar, et al., 2020) of renewable energy sources, they are considered as a best option to meet the fast growing demand for electrical energy worldwide. Among other renewable energy sources, photovoltaic (PV) energy is now becoming one of the fastest growing renewable energy technologies (Owusu, et al., 2016 and Gielen, et al., 2019). This is as a result of continuous cost reduction and technological progress achieved so far. PV is the field of technology related to the application of solar cells for energy by converting sunlight directly into electricity. Some merits of PV technology include low cost of operation, no environmental impact and less cost of maintenance. Also, some of the demerits are as follows: high installation cost, intermittence on the energy production, low efficiency, mismatch between the operating characteristics of the load and the PV array, etc (Husian, et al., 2018 and Chowdhury, et al., 2020).

Due to the non-linear characteristics of the PV panel it requires a maximum power point tracking (MPPT) algorithm (Dasgupta, et al., 2008, Lopez Lapena, et al., 2010 Esram, et al., 2007, Enslin, et al., 1997, Veerachary, et al., 2003 and Bialasiewicz, et al., 2006). Another drawback is the unequal power produced between the PV panels due to various factors, such as dissimilarities of panel production, different temperatures and irradiations due to the orientation of the panels, aging and shading. To design a PV system, solar cells are

packaged in PV modules and then connected to electronic converters. These modules are electrically connected in multiples as PV panel. The PV module exhibits a nonlinear voltage – current characteristic. Its maximum power point depends on irradiance and temperature (Nadia et al., 2020 and Ramos-Hernanz et al., 2020). At a particular solar irradiation, there is a unique operating point which coincides with the PV generator maximum output power. When sunshine is not consistent voltage and current output of a PV module is also affected and hence reduces the efficiency. To get maximum utilization efficiency of a PV module, the matching of the PV module to the load is required (Ayoub, et al., 2018 and Omar et al., 2021). This matching requires finding an equilibrium operating point which coincides with the maximum power point of the PV module.

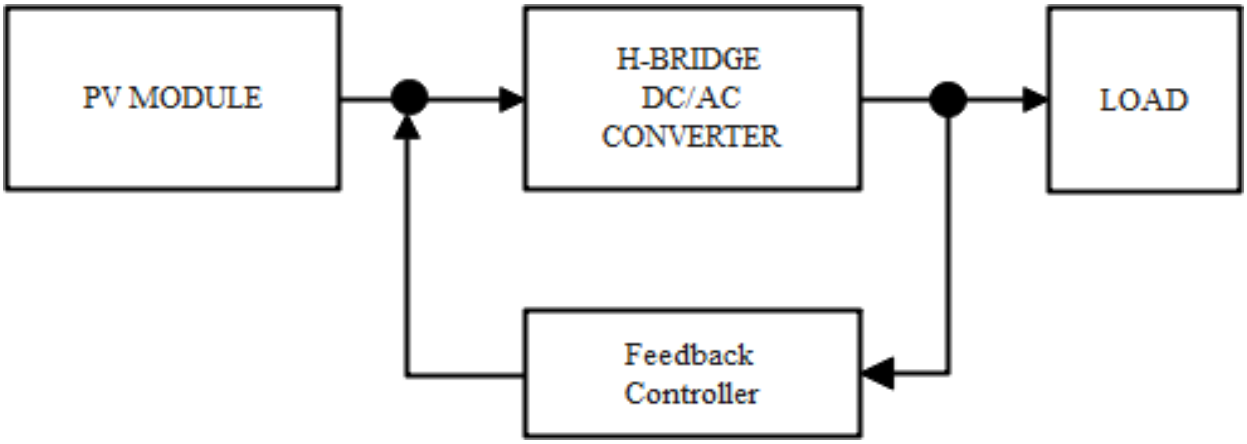

Figure 1: Block diagram of the complete system

DC-AC converter converts unregulated output DC voltage from PV cells to a regulated AC output voltage. For this conversion a highly efficient DC-AC converter is required. The solar energy conversion system provides the complete utilization of the solar energy. The DC – AC converter is adopted due to its advantages, ranging from low power switches to simple control method. The unregulated DC voltage generated from the PV module is due to variation of sun irradiance. This voltage is fed to the inverter power circuit which converts it to AC voltage (Oliveira, et al., 2012 and Khairy Sayed, et al., 2022). To enhance the efficiency of the output voltage, a resonant circuit (LC) filter is required (Mahalakshmi, et al., 2015). As a result of this PV voltage variation, proportional integral (PI) feedback controller is adopted to keep the output voltage constant.

An application of H-bridge voltage source inverter topology in sustainable energy system is investigated (Suresh et al., 2014 and Trimukhe, et al., 2021). In this paper, application of h-bridge voltage source inverter topology with proportional integral controller in a photovoltaic power conditioning system is investigated. The PV module consists of two input variables namely sun irradiance and temperature. The DC - AC conversion with respect to H-bridge voltage source inverter for stand-alone with resistive load is done. The performance of conventional inverter is compared and analyzed with respect to open loop and closed loop (using PI controller) considering output voltage, current, total harmonic distortion (THD) and power quality of the system. The effectiveness of the convectional H-bridge inverter topology is tested under sun irradiance variation at a constant temperature. A computer based simulation is carried out under MATLAB/SIMULINK using power system tool box.

2. MATERIAL AND METHODS

The complete system of the proposed H-bridge voltage source inverter for sustainable energy application consists of the PV module and feedback control system. A photovoltaic cell is a diode which is designed to promote the photovoltaic effect. The term PV denotes the unbiased operating mode of a photodiode in which current through the device is entirely due to the transduced light energy. The photovoltaic systems convert solar energy into electrical energy. It is a nonpolluting source of electricity and is highly reliable, which is suited for many applications. The solar cell is represented by a current source, a Shockley diode and a resistor as shown in Figure. 2. The current source generates a current proportional to the irradiation G [W/m^2]. The photo current, I_v is in turn directly proportional to the radiation level.

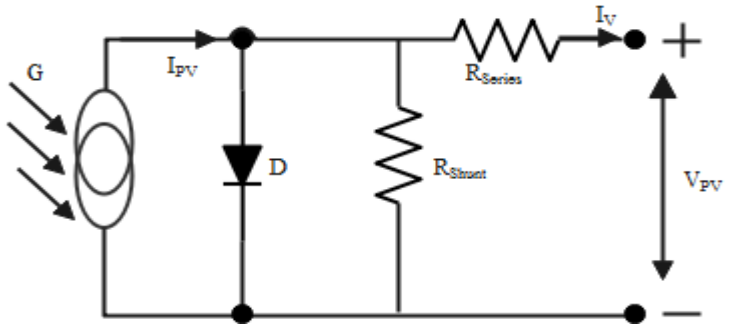

Figure 2: Equivalent Circuit of Solar Cell

The model of a PV module is developed for simulating an entire PV array; A PV module is made of many series connected PV cells.

A dc/ac converter acts as an interface between the load and the PV module as depicted in Figure 1. The circuit topology is made up of two (2)-level inverter legs supplied by one dc voltage source (V_{pv}), L_f - C_f filter connected at points 'a' and 'b', and a resistive load, R_o. The voltage drop across points 'a' and 'b' has a maximum of three levels $+V_{pv}$, 0 and $-V_{pv}$, thus when passed through an LC filter a pure sinusoidal output voltage and current are generated. Due to the nature of the load the output voltage and current are in-phase.

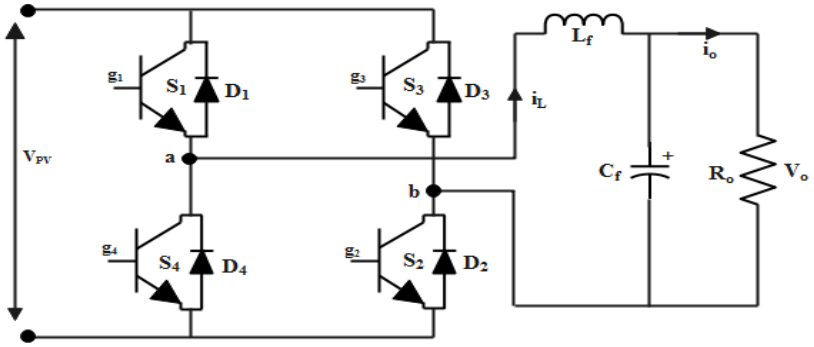

Figure 3: H-bridge dc-ac converter

The combination of power switches $S_1$and S_3 or S_2 and S_4 generates zero output voltage across ab while D_1 and D_3 or D_2 and D_4 serve as returning current paths respectively. The combination of switches S_1 and S_2 generates positive V_{pv} across point 'ab', while D_1 and D_2 serve as returning current paths. Further combination of switches S_3 and S_4 yields a negative V_{pv} across point ab, while D_3 and D_4 serve as the current returning paths during this operation.

Pulse width modulation with unipolar switching method is adopted as shown in Figure 4, for generating the firing signals for the four power switches in Figure 3. It consists of two control or reference signals operating at a fundamental frequency and one carrier triangular signal operating at a very high frequency. Here, the legs 'a' and 'b' of the full-bridge inverter are controlled separately by comparing V_{tri} with $V_{control}$ and $-V_{control}$, respectively.

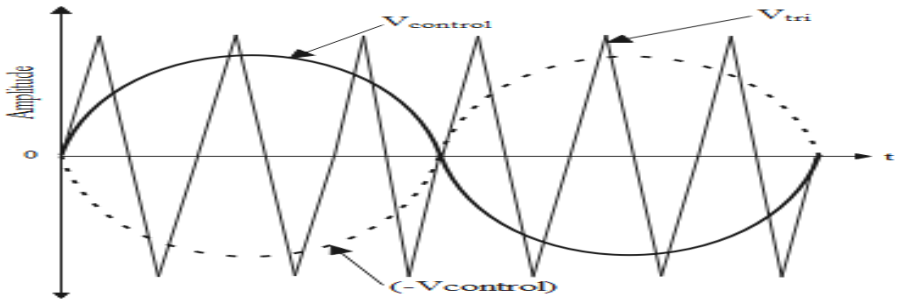

Figure 4: Pulse width modulation Scheme

As shown in Figure 4, the comparison of $V_{control}$ with triangular waveform results in the following logic signals to control the power switches in leg 'a'

$$\left.\begin{aligned} V_{control} > V_{tri} : g_1 = ON \; and \quad V_a = V_{PV} \\ V_{control} < V_{tri} : g_4 = ON \;\; \text{and} \quad V_a = 0 \end{aligned}\right\} \tag{1}$$

For controlling the leg 'b' switches, $-V_{control}$ is compared with the same triangular waveform, which yields the following:

$$\left.\begin{aligned} (-V_{control}) > V_{tri} : g_3 = ON \; and \quad V_b = V_{PV} \\ (-V_{control}) < V_{tri} : g_2 = ON \;\; \text{and} \quad V_b = 0 \end{aligned}\right\} \tag{2}$$

The four modes of operation of the inverter circuit is as summarized in Eqn. (3) with their corresponding voltage levels

$$\left.\begin{aligned} &1.\;\; g_1, g_2 = ON; \quad V_a = V_{PV}; \quad V_b = 0; \quad V_{ab} = V_{PV}; \\ &2.\;\; g_4, g_3 = ON; \quad V_a = 0; \quad V_b = V_{PV}; \quad V_{ab} = -V_{PV}; \\ &3.\;\; g_1, g_3 = ON; \quad V_a = V_{PV}; \quad V_b = V_{PV}; \quad V_{ab} = 0; \\ &4.\;\; g_4, g_2 = ON; \quad V_a = 0; \quad V_b = 0; \quad V_{ab} = 0; \end{aligned}\right\} \tag{3}$$

In this type of PWM control scheme, when a switching occurs, the output voltage changes between zero and $+V_{pv}$ or between zero and $-V_{pv}$ voltage levels. This type of control scheme called unipolar voltage switching has a better total harmonic distortion when compared with the bipolar voltage switching method.
Here, the output voltage, current and the inductor current are sensed to keep the output voltage constant at a reference value. As a result of this, the error generated between the reference voltage and output voltage is fed to the first PI controller system A. The resultant value from the PI controller A is added to the output current,

consequently, a second error result is generated from comparing the inductor voltage value. Then, this is passed through the second PI controller system B, and another error value is generated by comparing the output voltage value. Furthermore, a gain value K1 is used to scale down the generated error value and results to a control signal, $V_{control}$ while the gain block K2 generates another control signal, $-V_{control}$. This control adjusts the duty cycle of the system. At this juncture, a high frequency carrier signal, V_{tri} is introduced as depicted in Figure 5; the gating signal g1 is generated by comparing $V_{control}$ and V_{tri} using a comparator, CM1. In this same way, the gating signal, g_3 is generated by comparing $-V_{control}$ and V_{tri} using comparator CM2. The firing signals g_4 and g_2 are formed by negating g_1 and g_3 respectively. The PI loops operate with a much faster rate and provide fast response and overall system stability.

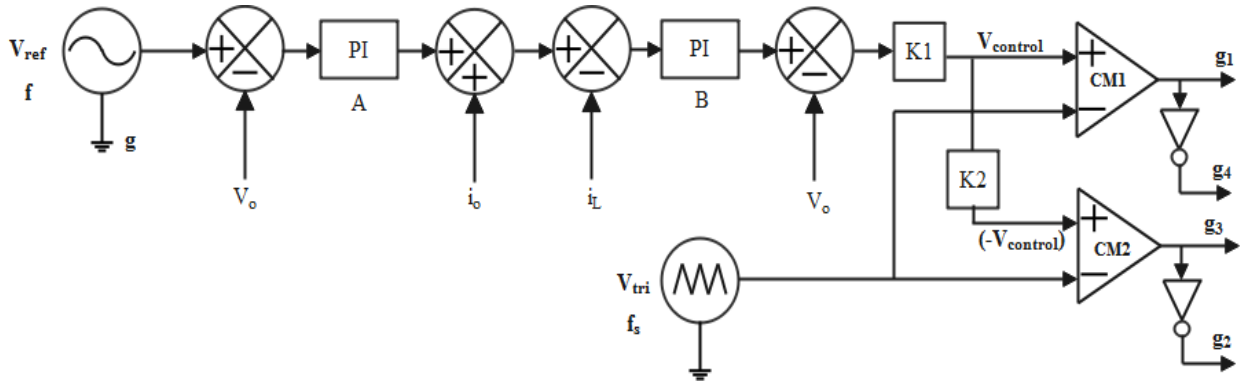

Figure 5: Feedback control technique

The connection of the Figures 2 -5 gives the internal configuration of the block diagram as depicted in Figure 1. From Figure 2; the solar – induced current can be calculated by (Gow, et al., 1999). Furthermore, the output voltage of the solar cell is then linked to the H-bridge inverter as V_{pv}, as indicated in Figure 3. The detailed mathematical analysis of H-bridge inverter is given in (Hasan, et al., 2015 and Anoopkumar et al., 2018). Therefore, the voltage drop across V_{ab} is given by (Rashid, 2004) as

$$V_{ab} = V_{pv}\sqrt{\sum_{k=1}^{2p}\frac{\delta_k}{\pi}} \tag{4}$$

where p is the number of pulses, δ_k is the pulse angle.

The mathematical expression of the PI controllers as depicted in Figure 5, can be written as

$$G_{cA}(s) = K_{pA} + \frac{K_{IA}}{s} \quad \text{and} \quad G_{cB}(s) = K_{pB} + \frac{K_{IB}}{s} \tag{5}$$

where K_{pA} is the gain of the proportional term of A, K_{IA} is the gain of the integral term of A, K_{pB} is the gain of the proportional term of B, K_{IB} is the gain of the integral term of B.

3. SIMULATION RESULTS

The system simulation performance analysis is categorized into two namely: open loop and closed loop performances. The PV system is modeled in the MATLAB/Simpower systems, it consists of one parallel connected PV arrays each array is made up of fourteen series connected PV assemblies. The module data can be extracted from Trina Solar TSM-315PA14A.08 module. The output of this PV module is given to the Full Bridge DC - AC converter with L_F and C_F filter values of 4.06 mH and 6.23 uF respectively. A resistive load of 55 ohms is used for the simulation purpose. The feedback controller is designed with PI controller to track

maximum power output and output voltage regulation with variation of load. Different parameters used are: Switching frequency - 10 k Hz, K_{pA} – 0.03115, K_{IA} – 0.03115/21, K_{pB} – 27.066, K_{IB} – 27.066/6.67, K1 – 1/400, and K2 – -1. Then, the reference voltage is 300 V at fundamental frequency of 50 Hz.

3.1 *Open Loop Results*

The proposed system is connected to the single-phase resistive load of 55 ohms. Figure 6 shows the variation of sun irradiance from 250 W/m^2, 750 W/m^2, 400 W/m^2, 650 W/m^2, and 500 W/m^2 for 2 secs with a constant temperature of 25^{0}C. The solar induced and diode currents are displayed in Figure 7. Figures 8 and 9 show the waveform of solar output voltage and three dimensional plot of current, voltage and time respectively.

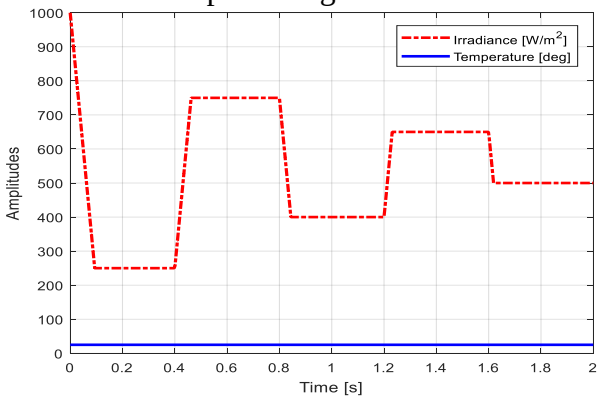

Figure 6: Waveforms of irradiance and temperature.

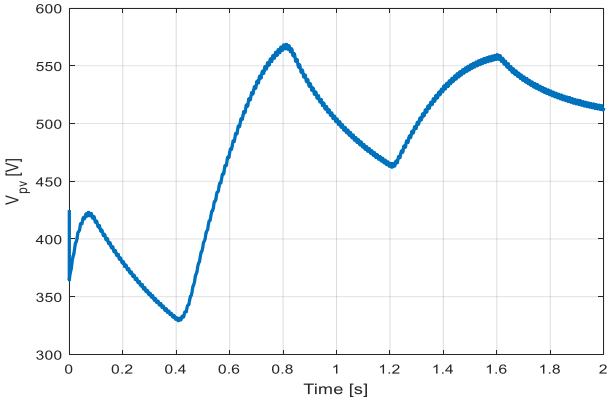

Figure 8: Waveforms of solar cell output voltage

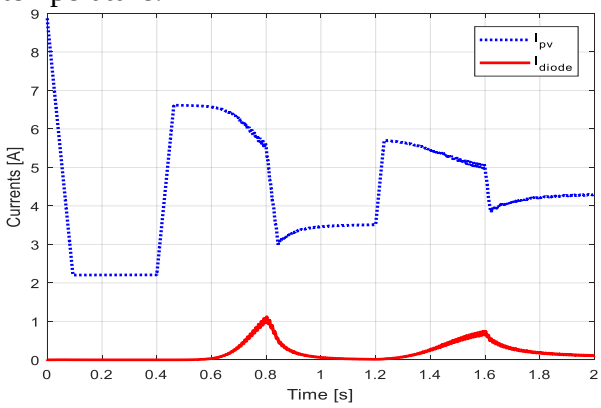

Figure 7: Waveforms of output solar induced and diode currents.

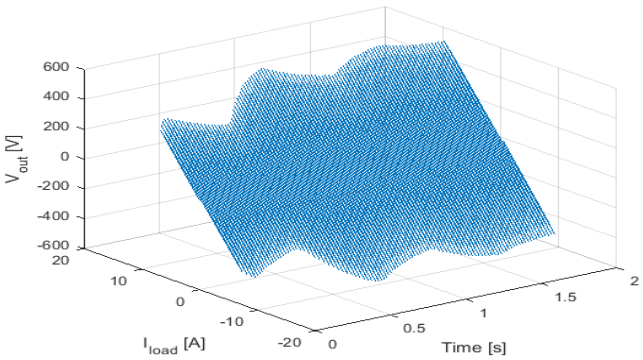

Figure 9: Three dimensional waveform of time, outputs current and voltage.

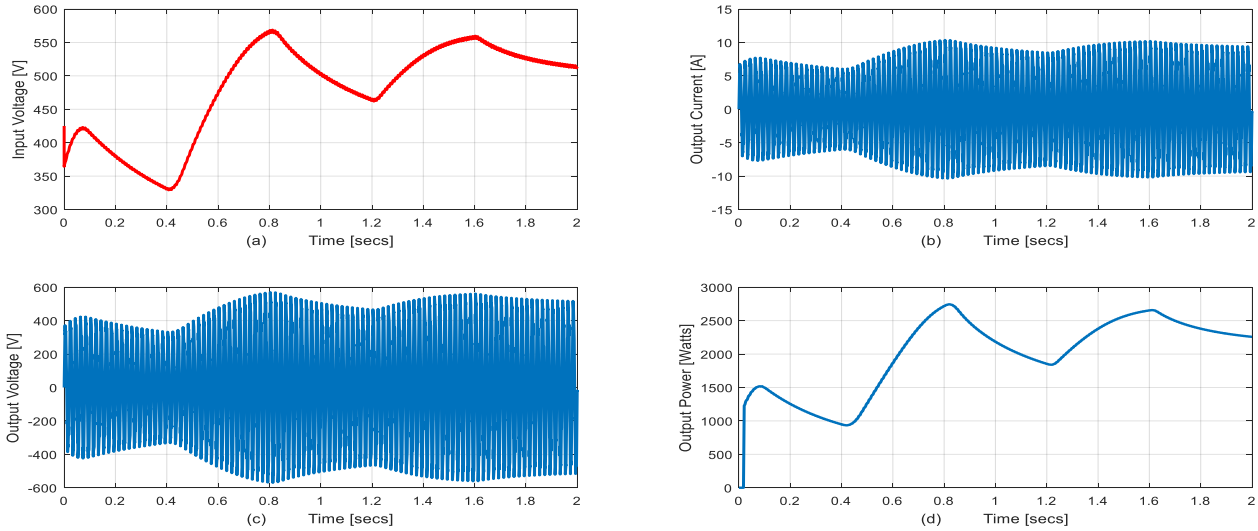

Figure 10: Waveforms of (a) inverter input voltage, (b) system output current, (c) system output voltage and (d) system output power.

It can be observed that the variation in the sun irradiance affects the solar cell output as indicated in Figure 10(a), the load current, voltage and power ratings are also affected by this parameter fluctuation as depicted in Figure 10 (b, c & d). It can be observed in Figure 11 that the waveforms of load voltage and current per three cycles are plotted, while Figure 12 shows the waveform of the harmonic profile. The readings of the voltage and current is taken between 1.50 secs to 1.56 secs, 500 V of load voltage is obtained while 10 A of load current is also obtained. The two waveforms are in-phase due to resistive loading of 55 ohms. A voltage THD value of 8.56 % and rms voltage value of 431.1 V are obtained for 20 harmonic orders.

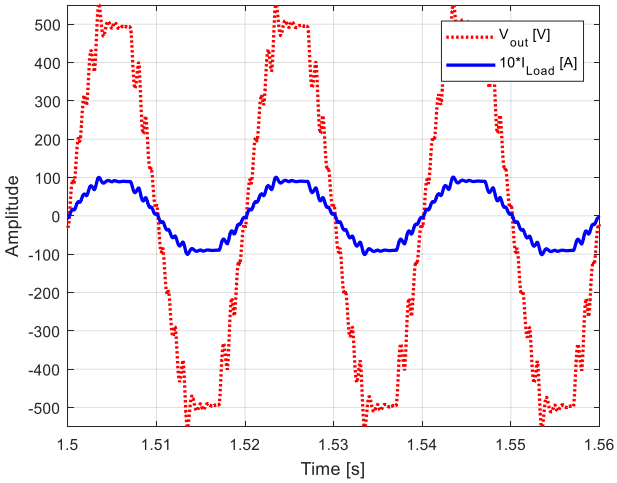

Figure 11: Waveforms of output current and voltage for three cycles.

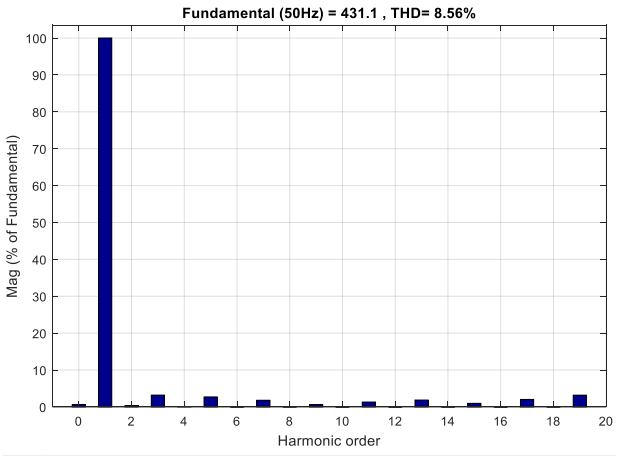

Figure 12: Harmonic profile of the system output voltage.

3.2 Closed Loop Results

Figure 13 depicts the waveforms of the irradiance and temperature under closed loop control simulation. The solar induced and diode currents are displayed in Figure 14. Figures 15 and 16 show the waveforms of solar output voltage and three dimensional plot of current, voltage and time respectively.

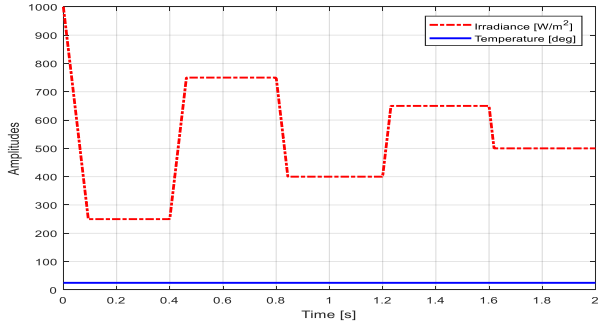

Figure 13: Waveforms of irradiance and temperature under closed loop.

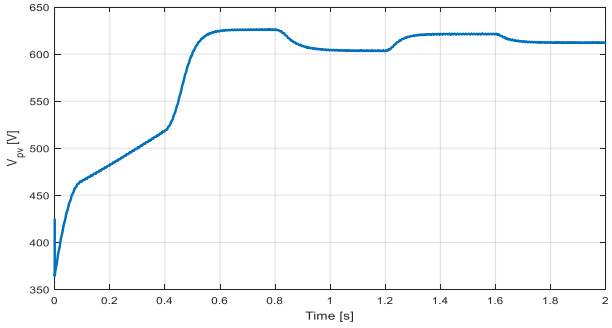

Figure 15: Waveforms of solar cell output voltage under closed loop.

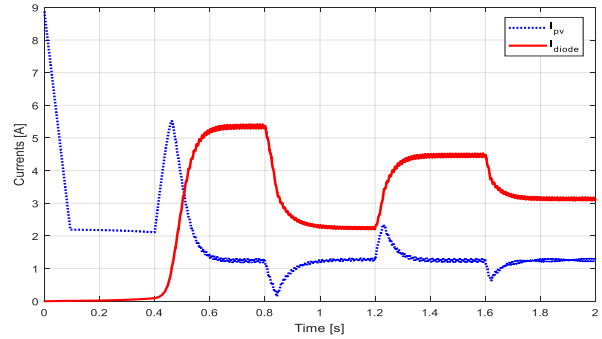

Figure 14: Waveforms of output solar cell and diode currents under closed loop

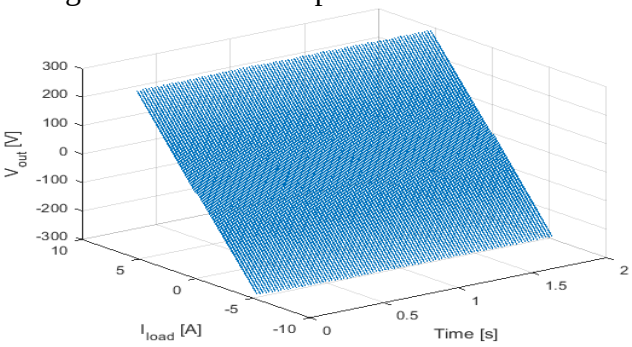

Figure 16: Three dimensional waveform of time, outputs current and voltage under closed loop

It can be observed that the variation in the sun irradiance affects the solar cell output as indicated in Figure 17(a), and the load current, voltage and power ratings are not affected by this parameter fluctuation as depicted in Figure 17 (b, c & d) due to the feedback control system that is introduced in the system. A constant power rating of 780 Watts is obtained.

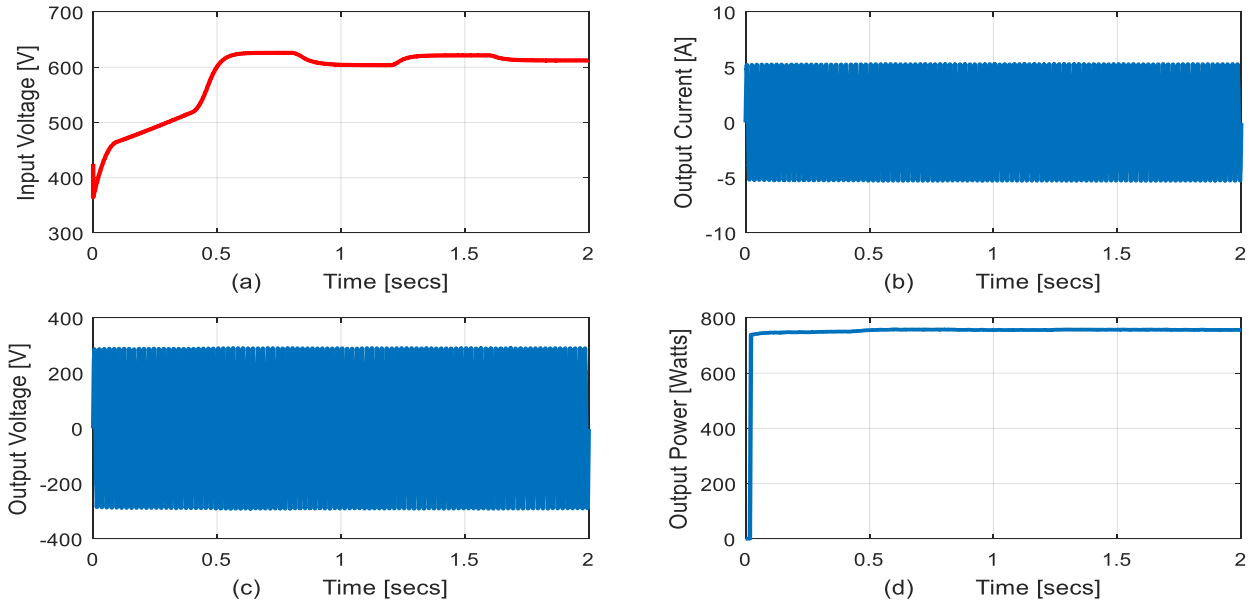

Figure 17: Waveforms of (a) inverter input voltage, (b) system output current, (c) system output voltage and (d) system output power under closed loop.

It can be observed in Figures 18 & 19 the waveforms of load voltage and current per three cycles and harmonic profile. The readings of the voltage and current is taken between 1.50 secs to 1.56 secs, 280 V of load voltage is obtained while 5 A of load current is also obtained. The two waveforms are in-phase due to resistive loading of 55 ohms. A voltage THD value of 0.97 % and rms voltage value of 288.5 V are obtained for 20 harmonic orders.

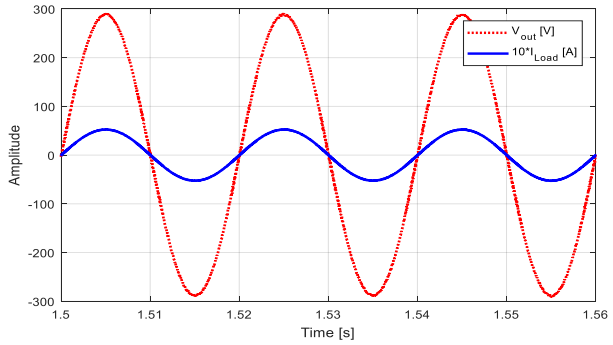

Figure 18: Waveforms of output current and voltage for three cycles under closed loop.

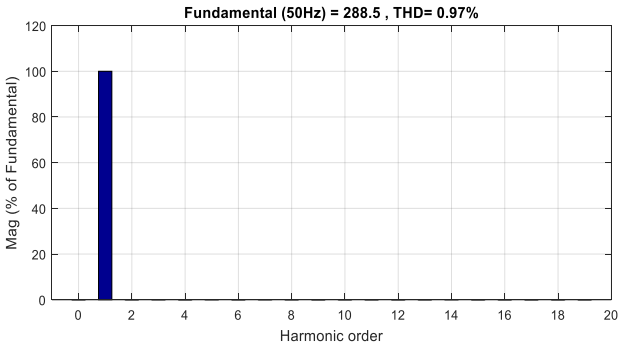

Figure 19: Harmonic profile of the system output voltage under closed loop.

4. CONCLUSIONS

In this paper, an application of H-bridge voltage source inverter topology in sustainable energy system is simulated. Also a novel feedback PI controller has been built using MATLAB/SIMULINK and its performance and efficiency is evaluated. It is found that for both open loop and closed loop performance outcome, the feedback system showed a good performance when compared with the open loop system. The system configuration is achieved by using only one stage conversion network; in addition, less power losses and circuit components are realized. As a result of the feedback system, a constant output power, high efficiency value of 99.49 % and voltage are achieved with low THD value of 0.97 %.

REFERENCES

Abolhosseini, S., Heshmatic, A. and Altmann, J. (2014). A Review of Renewable Energy Supply and Energy Efficiency Technology. IZA Discussion Paper No. 8145. https://ftp.iza.org/dp8145.pdf.

Adelakun O. and Olanipekun, B. A. (2019). A Review of Solar Energy. Journal of Multidisciplinary Engineering Science and Technology (JMEST). Vol. 6, Issue 12 pp. 11344-11347 www.jmest.org.

Anoopkumar M. V. and Sundaramoorthi P. A. (2018). Performance Analysis of H-Bridge Inverter Integrated For Renewable Energy Sources. International Journal on Future Revolution in Computer Science & Communication Engineering. Vol: 4 Issue: 4 pp. 550 – 552. https://www.researchgate.net/publication/330225575_Performance_Analysis_of_H_Bridge_Inverter_Integrated_For_Renewable_Energy_Sources [accessed Mar 31 2022].

Ansari, M. F., Chatterji, S., and Iqbal, A. (2010). A fuzzy logic control scheme for a solar photovoltaic system for a maximum power point tracker. Int. J Sustainable Energy, vol. 29, no. 4, pp. 245-255.

Ayoub, U. and Channi, H. (2018). Review on various strategies for maximum efficiency of solar panels. International Journal of Engineering and Technology. Vol. 7(2.12), pp. 266-267. www.sciencepubco.com/index.php/IJET.

Bialasiewicz, J. T. and E. Muljadi, E. (2006). Simulation-based analysis of renewable energy systems," IEEE Trans. Ind. Electron.,vol. 53, no. 4, pp. 1137-1143.

Brunton, S., Rowley, C., Kulkarni, S. and Clarkson, C. (2010). Maximum power point tracking for photovoltaic optimization using ripple-based extremum seeking control. IEEE Trans. Power Electron., vol. 25, no. 10, pp. 2531-2540.

Chen, L. R., Tsai, C. H., Lin, Y. L. and Lai, Y. S. (2010). A biological swann chasing algorithm for tracking the PV maximum power point. IEEE Trans. Energy Convers., vol. 25, no. 2, pp. 484- 493.

Chowdhury, M.S., Rahman, K. S., Chowdhury, T., Nuthammachot, N., Techato, K., Akhtaruzzaman, M., Tiong, S. T., Sopian, K. and Amin, N. (2020). An overview of solar photovoltaic panels' end-of-life material recycling". Elsevier Energy Strategy Reviews. Vol. 27 100431. https://doi.org/10.1016/j.esr.2019.100431.

Dasgupta, N., Pandey, A. and Mukeziee, A. (2008). Voltage-sensing based photovoltaic MPPT with improved tracking and drift avoidance capabilities," Solar Energy Mater. Solar Cells, vol. 92, no. 12, pp. 1552-1558.

Emeghara, M. C., Obi, P. I. and Onah, A. J. (2022). Modeling and Performance Evaluation of a Hybrid Solar-Wind Power Generation Plant. Journal of Energy Technology and Environment. Vol. 4(1), pp. 21-28. www.nipesjournal.org.ng.

Enslin, J. H. R., Wolt, M. S., Snyman, D. B. and W Swiegers, W. (1997). Integrated photovoltaic maximum power point tracking converter," IEEE Trans. Ind. Electron., vol. 44, no. 6, pp. 769- 773.

Esram T. and Chapman, P. (2007). Comparison of photo voltaic array maximum power point tracking techniques. IEEE Trans. Energy Convers., vol. 22, no. 2, pp. 439-449.

Gielen, D., Boshell, F., Saygin, D., Bazillian, M. D., Wagner, N and Gorini, R. (2019). The role of renewable energy in the global energy transformation. Elsevier Energy Strategy Reviews. Vol. 24 pp. 38-50. https://doi.org/10.1016/j.esr.2019.01.006.

Gow, J.A. and Manning, C. D. (1999). Development of a Photovoltaic Array Model for Use in Power-Electronics Simulation Studies." IEEE Proceedings of Electric Power Applications, Vol. 146, No. 2, pp. 193–200.

Gul, M. Kotak, Y. and Muneer, T. (2016). Review on Recent Trend for Solar Photovoltaic technology. Sage Journals – Energy Exploration and Exploitation. https://doi.org/10.1177/0144598716650552.

Hasan Komurcugil, Necmi Altin, Saban Ozdemir, and Ibrahim Sefa, (2015). An Extended Lyapunov-Function-Based Control Strategy for Single-Phase UPS Inverters," IEEE Transactions On Power Electronics, Vol. 30, No.7.

Husian, A. A. F., Hasan, W. Z. W., Shafie, S., Hamidon, M. N. and Pandey, S. S. (2018). A review of transparent solar photovoltaic technologies. Elsevier Renewable and Sustainable Energy Reviews. Vol. 94, pp. 779-791. Oct. 2018. https://doi.org/10.1016/j.rser.2018.06.031.

Juraz, J., Canales, F. A., Kies, A., Guezgouz, M. and A. Beluco (2020). A Review on the complementarity of renewable energy sources: Concept, metrics, applications and future research direction. Elsevier Solar Energy Vol. 195, pp. 703-724. https://doi.org/10.1016/j.solener.2019.11.087.

Khairy Sayed, Abdulaziz Almutairi, Naif Albagami, Omar Alrumayh, Ahmed G. Abo-Khalil and Hedra Saleeb (2022). A Review of DC-AC Converters for Electric Vehicle Applications. Energies 2022, 15(3), 1241; https://doi.org/10.3390/en15031241

Kumar, J. C.R. and Majid, M. A. (2020). Renewable energy for sustainable development in India: current status, future prospects, challenges, employment, and investment opportunities. Energy Sustain Soc. 10**,** 2. https://doi.org/10.1186/s13705-019-0232-1

Lopez Lapena, O., Penella, M. and Gasulla, M. (2010). A new MPPT method for low-power solar energy harvesting. IEEE Trans. Ind. Electron., vol. 57, no. 9, pp. 3129-3138.

Mahalakshmi, R and Sindhu Thampatty, K. C. (2015). Grid Connected Multilevel Inverter for Renewable Energy Applications," Procedia Technology, vol. 2, pp. 636 – 642.

Nadia, M., Lassad, H., Zaafouri, A and Abdelkader, C. (2020). Influence of Temperature and irradiance on the different solar PV panel technologies. International Journal of Energy Sector Management. Doi: 10.1108/IJESM-06-2020-0002.

Nagaiah, M., Chaitanya Krishna, J., and Shaik Rafi Kiran (2017). Application of Multilevel Inverters in Solar, Battery and Wind hybrid System for Domestic Load Application. International Journal of Advanced Engineering Research and Science (IJAERS), pp. 1- 5. https://dx.doi.org/10.22161/ijaers/nctet.2017.eee.1

NingYi Dai, Chi-Seng Lam, and WenChen Zhang (2014). Multifunctional Voltage Source Inverter for Renewable Energy Integration and Power Quality Conditioning. Hindawi Publishing Corporation The Scientific World Journal, pp. 1-10. http://dx.doi.org/10.1155/2014/421628

Oliveira, J. G., Schettino, H., Gama, V., Carvalho, R and Bernhoff, H. (2012). Implementation and Control of an AC/DC/AC Converter for Double Wound Flywheel Application. Advances in Power Electronics, vol. 2012, Article ID 604703, 8 pages. https://doi.org/10.1155/2012/604703.

Omar, M. A., & Mahmoud, M. M. (2021). Improvement Approach for Matching PV-array and Inverter of Grid Connected PV Systems Verified by a Case Study. International Journal of Renewable Energy Development, 10(4), 687-697. https://doi.org/10.14710/ijred.2021.36082

Owusu, P. A. and Asumadu-Sarkodie, S. (2016). A review of renewable energy sources, sustainability issues and climate change mitigation. Cogent Engineering, Vol. 3, Issue 1. https://doi.org/10.1080/23311916.2016.1167990.

Ramos-Hernanz, J., Uriarte, I. and Lopez-Guede, J. M. (2020). Temperature based maximum power point tracking for photovoltaic modules. Sci Rep 10, 12476. https://doi.org/10.1038/s41598-020-69365-5

Rashid, M. H. (2004). Power electronics circuits, devices and applications. Prentice-Hall of India Private Limited, New Delhi, pp. 233, 2004.

Sujatha, M. and Parvathy, A. K. (2019). Improved reliable multilevel inverter for renewable energy systems. Indonesian Journal of Electrical Engineering and Computer Science, Vol. 14, No. 3, pp. 1141~1147 ISSN: 2502-4752, DOI: 10.11591/ijeecs.v14.i3.

Suresh, S., Kannan, S. and Sundaravel, S. P. (2014). A modified Single phase H-Bridge Inverter for High Power Application with Power Quality Improvement. Applied Mechanics and Materials. Vol. 626, pp. 118-126. Trans Tech Publications, Switzerland. Doi: 10.4028/ www.scientific.net/AMM.626.118.

Trimukhe, S. and Sanjeevkumar, R. A. (2021). Grid interconnected H-bridge Multilevel Inverter for renewable power applications using Repeating Units and Level Boosting Network. Global Transitions Proceedings. https://doi.org/10.1016/j.gltp.2021.10.005. Accessed 30/03/2022.

Veerachary, M., Senjyu, T. and Uezato, K. (2003). Maximum power point tracking of coupled inductor interleaved boost converter supplied PV system", lEE Proc. -Electr. Power Appl., vol. 150, no. I, pp. 71-80.